System reliability analysis of layered soil slopes using fully specified slip surfaces and genetic algorithms

Peng Zeng , Rafael Jimenez , Rafael Jurado-Piña

A B S T R A C T

This paper presents a new approach to identify the fully specified representative slip surfaces (RSSs) of layered soil slopes and to compute their system probability of failure, $P_{f,s}$. Spencer's method is used to compute the factors of safety of trial slip surfaces, and the first order reliability method (FORM) is employed to efficiently evaluate their reliability. A custom-designed genetic algorithm (GA) is developed to search all the RSSs in only one GA optimization. Taking advantage of the system aspects of the problem, such RSSs are then employed to estimate the reliability of the slope system, and a proposed linearization approach—based on first or second order (FORM or SORM) reliability information about the identified RSSs—is used to efficiently estimate $P_{f,s}$. Three typical benchmark-slopes with layered soils are adopted to demonstrate the efficiency, accuracy and robustness of the suggested procedure, and advantages of the proposed method with respect to alternative methods are discussed. Results show that the proposed approach provides reliability estimates that improve previously published results, emphasizing the importance of finding good RSSs—and, especially, good (probabilistic) critical slip surfaces that might be circular or non-circular—to obtain good estimations of the reliability of soil slope systems.

Keywords:
Layered soil slope
System reliability
Representative slip surface
Genetic algorithms
Fully specified slip surface
FORM

1. Introduction

Probabilistic analyses of slope stability have become a topic of increasing interest in the geotechnical literature (see e.g., Oka and Wu, 1990; Chowdhury and Xu, 1993, 1995; Griffiths and Fenton, 2004; Hong and Roh, 2008; Ching et al., 2009; Cho, 2009; Ching et al., 2010; Huang et al., 2010; Low et al., 2011; Wang et al., 2011; Zhang et al., 2011; Ji and Low, 2012; Cho, 2013; Li et al., 2013; Zhang et al., 2013; Li and Chu, 2014; Li et al., 2014). Some studies have focused on the search for "critical" slip surfaces; i.e., slip surfaces with a minimum reliability index, β. But, as pointed out by Cornell (1971), slope stability is clearly a system problem: a slope may fail along many slip surfaces, and the probability of failure of the slope system, $P_{f,s}$, is larger than the probability of failure of any individual slip surface.

Simulation methods, such as Monte Carlo simulation (MCS) can naturally deal with the system aspects of slope stability to compute $P_{f,s}$. But they could be computationally expensive, particularly for slopes with small probabilities of failure (Ching et al., 2009). More efficient simulation methods, such as "subset simulation" (Wang et al., 2011) and Importance Sampling (IS) (Ching et al., 2009, 2010), have also been employed to solve the system's reliability problem. However, to obtain unbiased estimators of $P_{f,s}$, several previous approaches based on these simulation methods (see e.g., Ching et al., 2010; Wang et al., 2011) need to search the critical slip surface in many of the simulations conducted, hence significantly increasing their computational cost; whereas other approaches, to avoid the optimization problem of finding critical slip surfaces, are based on randomly generated trial slip surfaces (see e.g., Ching et al., 2009), which may therefore miss the critical one, hence providing biased estimators of $P_{f,s}$.

An alternative approach to overcome these drawbacks is to take advantage of the special nature of soil slopes. Zhang et al. (2011) pointed out that the factors of safety of potential slip surfaces are 'correlated'. $P_{f,s}$ can be therefore estimated considering only a few weakly correlated representative slip surfaces (RSSs); in particular, only those RSSs with a higher contribution to $P_{f,s}$ are needed.

The identification of the RSSs of a layered slope system is a challenging task, and several approaches have been therefore proposed to identify them. Some are based on randomly generating many potential slip surfaces (see e.g., Zhang et al., 2011; Li and Chu, 2014; Li et al., 2014), being again likely to miss the critical one; whereas others employ formal optimization methods—such as the extended Hassan and Wolff method (Ji and Low, 2012; Zhang et al., 2013) and the Broyden–Fletcher–Goldfarb–Shanno (BFGS) algorithm with barrier optimal method (Cho, 2013)—but mostly considering circular slip surfaces only. This means that they will often miss the critical slip surface, particularly in the presence of weak seams (see Zolfaghari et al., 2005); and missing the critical slip surface is likely to make them underestimate $P_{f,s}$. Some researchers have considered non-circular slip surfaces: Ching et al.

(2010) employed the procedure suggested in Greco (1996) to identify non-circular critical slip surfaces in weak seams; and Wang et al. (2011) mentioned that their method can be extended to consider non-circular slip surfaces. But as discussed above, these previous approaches could be computationally expensive. Similarly, Cho (2013) briefly described the use of non-circular slip surfaces in a horizontally-layered slope using the method in Kim and Lee (1997), but with an optimization algorithm that as we show later, failed to identify the critical slip surfaces. For those reasons, developing improved algorithms to identify the RSSs and to compute $P_{f,s}$ is still needed.

This paper presents a new approach to estimate the system's probability of failure of slopes in soils formed by layers with uncertain properties. (Spatial variability within layers is not considered.) The approach makes use of "fully specified slip surfaces". (The term "fully specified slip surface" is employed herein to denote slip surfaces—that could be circular or non-circular but with concave shape—whose geometry is described by the coordinates of all their individual nodes.) Our work extends the genetic algorithm (GA) designed by Jurado-Piña and Jimenez (2014) for the search of fully specified slip surfaces with minimum factor of safety, to consider that the fitness of trial slip surfaces is given by their reliability computed with the First Order Reliability Method (FORM); and it integrates such extended GA with a modified version of the algorithm proposed by Zhang et al. (2011), to select, during the search process, the RSSs that contribute most to the system reliability. A linearization approach is proposed so that the identified RSSs, together with their FORM reliability information, can be used to efficiently estimate the system probability of failure, $P_{f,s}$. Finally, the performance of the proposed method is tested using three different example cases based on typical benchmark-slopes from the literature, obtaining $P_{f,s}$ estimates that improve previously published results.

2. Reliability of slope systems

2.1. Introduction

The reliability of a slope in a layered soil can be modeled as a series system: i.e., as a system that fails when any of its 'components' (or possible slip surfaces) fails. An infinite number of slip surfaces is possible in theory, but only a few are needed to explain the overall $P_{f,s}$ — they are the representative slip surfaces, or RSSs. In our approach, the reliability analysis of a slope system requires three 'tools': (*i*) a first one to compute the performance of individual slip surfaces (i.e., their 'failure' or 'non-failure' states as given by their limit state functions, LSFs), and their reliability (i.e., their probability of failure) given an uncertain characterization of properties; (*ii*) a second one to identify the RSSs; and (*iii*) a third one to compute the reliability of the (series) system.

Methods employed in this paper as tools (*i*) and (*iii*)—i.e., to compute the reliability of an individual slip surface and of a series system—are discussed below. Section 3 describes the developed methodology employed as tool (*ii*); i.e., to identify the RSSs using a new GA approach.

2.2. Computing the reliability of an individual slip surface

Spencer's method, as implemented in SLOPE8R (Duncan and Song, 1984) with minor modifications to improve convergence, is used in this research to compute the factors of safety of slopes with fully specified slip surfaces. Spencer's method considers parallel inter-slice forces, satisfies both moment and force equilibrium, and is applicable to failure surfaces of any shape (circular and non-circular), hence being the "simplest of the complete equilibrium procedures for calculating the factor of safety" (Duncan and Wright, 2005).

For a slope with a set of given uncertain (random) input variables, $\mathbf{x}$, characterized by their joint probability density function (PDF), $f_{\mathbf{x}}(\mathbf{x})$, reliability methods aim to compute the probability of failure of the slope, as given by the following integral:

$$P_f = P\{G(\mathbf{x}) \le 0\} = \int_{G(\mathbf{x})\le 0} f_{\mathbf{x}}(\mathbf{x})d\mathbf{x} \tag{1}$$

where $G(\mathbf{x})$ is the limit state function of the slope, LSF, defined as $G(\mathbf{x}) = F_S(\mathbf{x}) - 1$, with F_S being the factor of safety of the slope computed with Spencer's method (note that $G(\mathbf{x}) \le 0$ indicates "failure").

Directly computing the integral in Eq. (1) is challenging, particularly when the LSFs are implicit. The first order reliability method (FORM) was developed to more easily solve Eq. (1). To that end, the original LSF in physical space can be transformed to the standard normal space (see Der Kiureghian (2005) for details), hence providing a transformed LSF, $g(\mathbf{u}) = 0$. Then, FORM uses a linear approximation to $g(\cdot) = 0$ at the "design point", $\mathbf{u}^*$, which can be obtained solving the following constrained optimization problem:

$$\begin{cases} \min\limits_{\mathbf{u}} \|\mathbf{u}\| \\ \text{subject to} \quad g(\mathbf{u}) = 0 \end{cases} \tag{2}$$

where $\|\cdot\|$ is the norm of a vector. Once $\mathbf{u}^*$ is obtained, its (minimum) distance to the origin is called the reliability index, $\beta = \|\mathbf{u}^*\|$, and the probability of failure can be computed as $P_f \approx \Phi(-\beta)$, where $\Phi(\cdot)$ is the cumulative distribution function (CDF) of the standard normal distribution.

Several algorithms have been proposed to find the design point that solves the FORM problem in Eq. (2) (see e.g., Hasofer and Lind, 1974; Rackwitz and Flessler, 1978; Santos et al., 2012). In this study, the improved Hasofer–Lind Rackwitz–Flessler (iHLRF) algorithm (Zhang and Der Kiureghian, 1995)—a tradeoff between efficiency and accuracy—is employed.

FORM also provides 'unit direction vectors' needed to compute correlations between the different LSFs involved in a system. In particular, the correlation coefficient between two LSFs (or slip surfaces), $\rho_{i,j}$, can be computed as $\boldsymbol{\alpha}_i^{\mathrm{T}}\boldsymbol{\alpha}_j$, where $\boldsymbol{\alpha}$ is the unit direction vector at the design point, given by $\boldsymbol{\alpha} = \mathbf{u}^*/\|\mathbf{u}^*\|$.

2.3. A linearization approach to compute the reliability of a series system

Whenever a set of m RSSs of a layered slope system are identified during the search process using the procedure proposed herein (see Section 3), the probability of failure of the series system can be estimated, efficiently and accurately, using the FORM-results (β and $\boldsymbol{\alpha}$) for the LSFs of the identified RSSs, as (Hohenbichler and Rackwitz, 1982; Zeng and Jimenez, 2014):

$$P_{f,s} = 1 - P^{1,\ldots,m} \approx 1 - \Phi_m(\boldsymbol{\beta}, \mathbf{R}) \tag{3}$$

where $P^{1,\ldots,m}$ is the probability of the intersection of safe domains for the m RSSs (and their associated LSFs) considered; $\Phi_m(\boldsymbol{\beta}, \mathbf{R})$ is the CDF of the m-dimensional standard normal distribution, evaluated at the vector of reliability indices, $\boldsymbol{\beta} = [\beta_1, \beta_2, \cdots, \beta_m]$, and with correlation matrix, $\mathbf{R}$, given by $\mathbf{R}[i,j] = \rho_{i,j}$, $i = 1, \ldots, m$ and $j = 1, \ldots, m$. (Φ_m is readily available in standard mathematical packages; for instance, it can be computed efficiently by MATLAB's pre-complied function **mvncdf**.) In general, the reliability index corresponding to the ith LSF, β_i, can be computed using FORM. Although, as we will see, reliability indices computed with the second order reliability method (SORM) (Phoon, 2008) improve the computed estimates of $P_{f,s}$ and might be needed when the LSFs are highly non-linear (Zeng and Jimenez, 2014) (note, however, that many slope stability problems are expected to be quite linear (see e.g., Zhang et al., 2011; Li and Chu, 2014; Zeng and Jimenez, 2014); for instance, the LSF associated to Bishop's simplified method for cohesive soils under short-term conditions and with normally distributed and uncorrelated cohesions is *exactly* linear).

3. A genetic algorithm approach to identify fully specified representative slip surfaces (RSSs)

Recent researches show that, with adequate encodings and operators, GAs can become a reliable and efficient tool to flexibly search for critical slip surfaces in deterministic slope stability analyses (Sun et al., 2008; Li et al., 2010; Jurado-Piña and Jimenez, 2014). The "general structure" of a common GA is shown in the left of Fig. 1. Given an initial population of 'individuals', or trial slip surfaces, the fittest ones (i.e., individuals that are better solutions, as measured by a problem-specific fitness function) have a higher probability of transmitting their features—through selection and reproduction operations—to

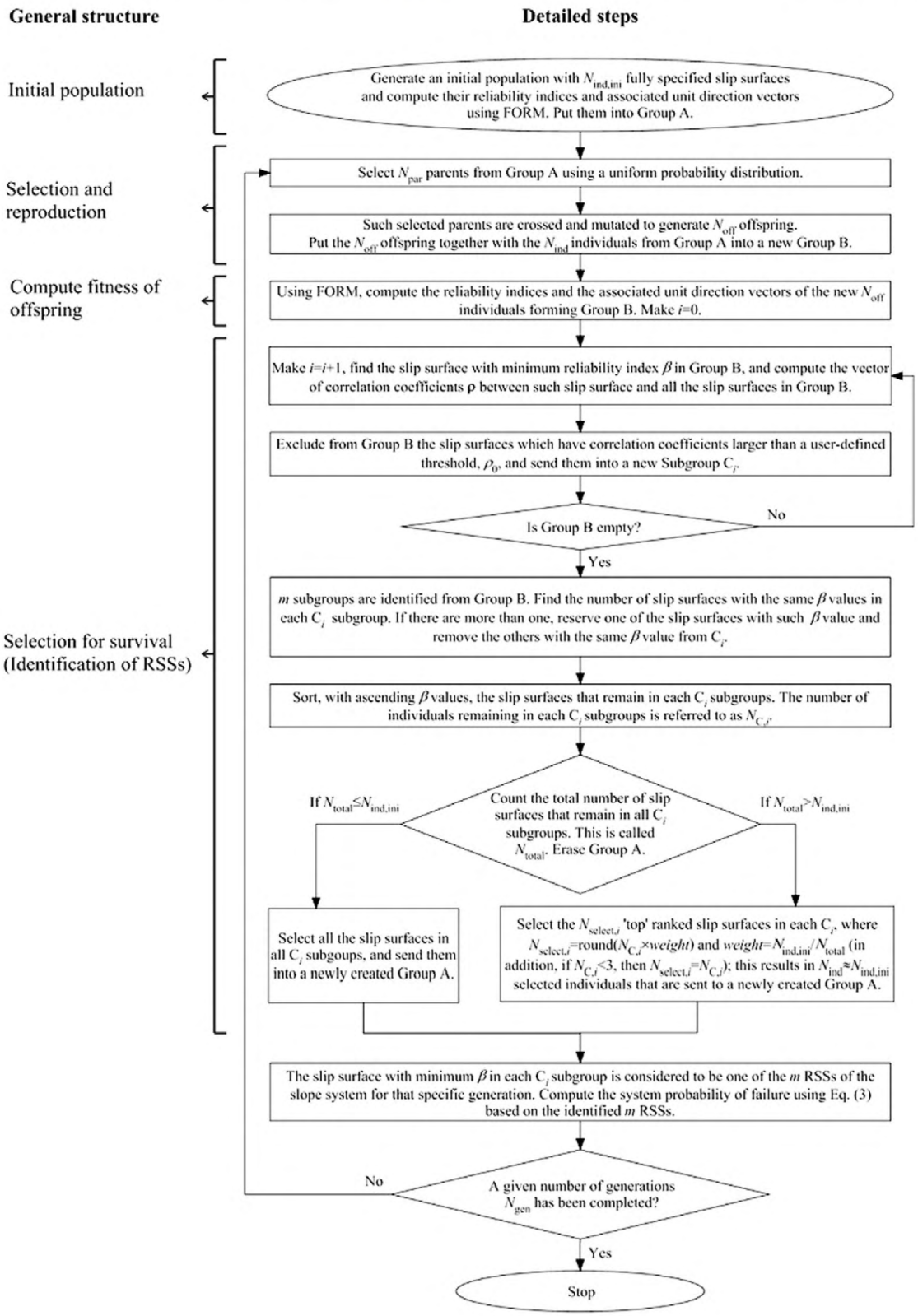

Fig. 1. A flowchart to illustrate the method of system reliability analysis using GAs.

forthcoming generations, therefore tending to improve them as solutions to the problem. This makes the population to evolve over successive generations so that it converges near the global optimum. In principle, the iterations continue for as long as the improvements are noticeable; however, a stopping criterion based on a minimum number of generations is also usually imposed to guarantee a good exploration and to prevent the solution from being trapped in a local minimum.

The right part of Fig. 1 shows a flowchart with "detailed steps" that the algorithm employs to search the RSSs. The proposed methodology builds on the custom-designed GA recently proposed by Jurado-Piña and Jimenez (2014) to solve (deterministic) slope stability problems. In particular, the fitness of individuals from a population of trial slip surfaces—which may be the initial population or an intermediate population in which offspring are obtained using the selection, mutation and crossover operators explained in Jurado-Piña and Jimenez (2014)—are simply obtained as their reliability indices computed with FORM. These FORM results (reliability indices and their associated unit direction vectors), computed for the whole population (parents with offspring), are then employed to identify the RSSs using a modification of the methodology proposed by Zhang et al. (2011). After selecting a group of slip surfaces from the whole population for survival, a new population is obtained and the full process is repeated. Finally, the system probability of failure of the slope is computed, with results obtained after applying the FORM (or SORM) to the identified RSSs, through the complementary of the intersection of safe domains summarized by Eq. (3).

Subsections below further explain the steps of this new procedure, providing additional details required for clarity. But, first, a description of how to represent (encode) a slip surface is needed.

3.1. Encoding of a trial slip surface

We consider "fully specified slip surfaces" as (open; two-dimensional) polygonal lines with N nodes ($N = 13$ is employed herein). The location of nodes is referred to a $[x,y]$ orthogonal system and nodes, V_i, are numbered sequentially (from 1 to N) from 'top to bottom' of the slope (see Fig. 2). The slip surface is completely defined with the coordinates of all its nodes within the considered reference system, which allows for a great flexibility of shapes and positions of the trial slip surfaces, including specific cases such as (quasi-)circular slip surfaces and planar slip surfaces (Krahn, 2004).

The locations of nodes, as well as the entry and exit angles of the slip surface, need to fulfill some restrictions. For instance, the 'extreme' nodes (i.e., V_1 or V_N) must lie within "allowable extreme intervals" defined by the analyst; the 'interior' nodes must also lie within an analyst-defined "allowable search domain"; and the trial slip surface considered must be upward-concave and kinematically feasible.

3.2. Initial population

The generation of the initial population follows the procedure described in Jurado-Piña and Jimenez (2014). A total of $N_{ind,ini}$ fully specified kinematically admissible slip surfaces are generated and stored in a group labeled "Group A". (Initial populations with $N_{ind,ini} = 100$ individuals are used herein.) Then, the 'fitness' of each slip surface of the initial population is evaluated based on their reliability indices, β, computed using FORM (see Section 2.2). The associated unit direction vectors, $\boldsymbol{\alpha}$, which are easily computed from the FORM solutions for each slip surface, are also recorded.

3.3. Selection and reproduction

The next step is to select parent slip surfaces from Group A using a uniform probability distribution, and to apply the mutation or crossover operators on them to obtain offspring. Our GA employs custom-designed operators for mutation and crossover that produce kinematically feasible slip surfaces with a high probability. Two crossover—heuristic crossover and arithmetic crossover—and eight mutation—uniform mutation of single node, non-uniform mutation of single node, total non-uniform mutation, straight mutation, 'extreme vertices' mutation, parabolic mutation, random lumped mutation and straight lumped mutation—operators are used. Crossover operators require two parents and mutation operators require only one. The arithmetic crossover operator produces two offspring, whereas all the other operators produce one. Further details of each operator can be found in Jurado-Piña and Jimenez (2014). We apply five times each of the two crossover and eight mutation operators, hence needing $N_{par} = 60$ parents to produce $N_{off} = 55$ new offspring. These newly generated N_{off} offspring, together with the N_{ind} individuals in Group A, are grouped together into a new group labeled "Group B" (Note that, as the algorithm evolves, N_{ind} may be slightly different to $N_{ind,ini}$. This is due to the way in which individuals are selected for survival; see Section 3.5).

3.4. Compute fitness of offspring

In this step, FORM is used to compute the reliability indices of the new N_{off} slip surfaces forming Group B. Such reliability indices will be employed later as a direct measure of 'fitness' in their selection for survival, as the lower the β of a slip surface, the better it is as a solution. The associated unit direction vectors are computed from the FORM solutions and recorded.

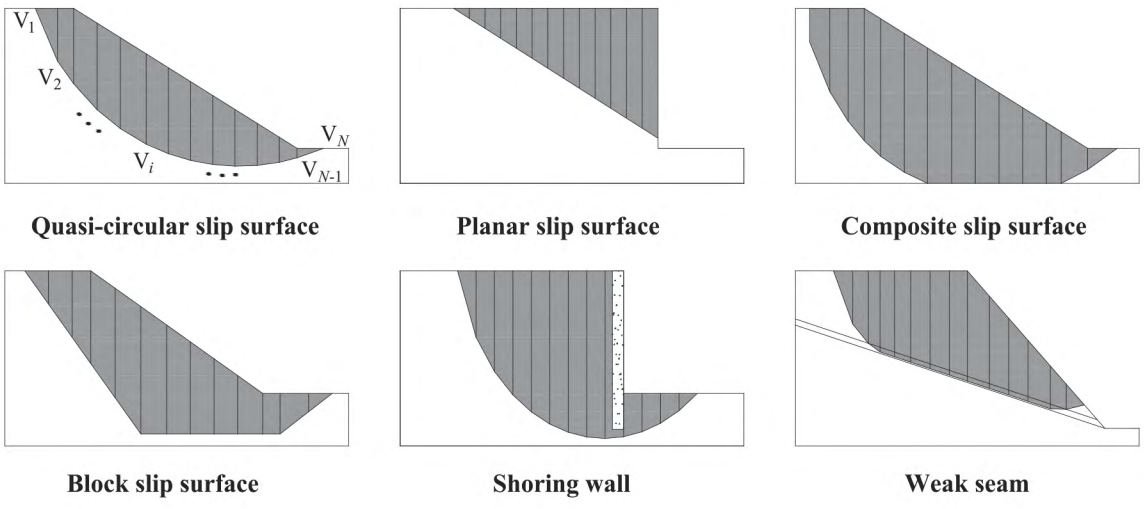

Fig. 2. Fully specified slip surfaces in different shapes and positions.

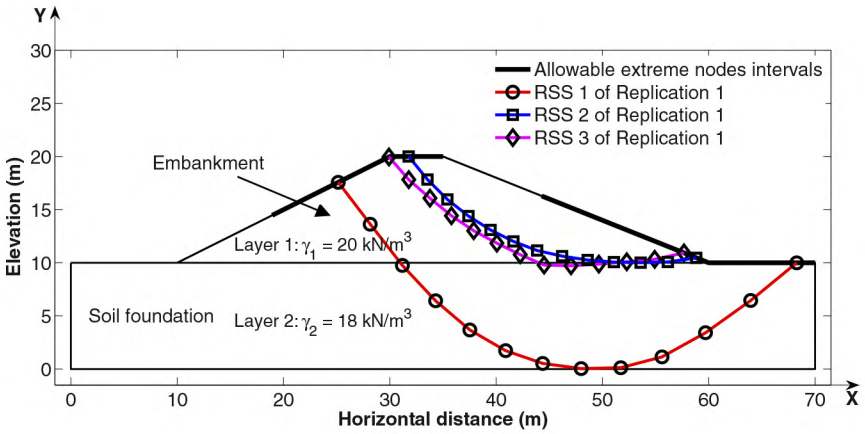

Fig. 3. Case 1. Geometry of a two layers soil slope and the RSSs identified in Replication 1.

3.5. Selection for survival: identification of RSSs

In this step the RSSs are identified from Group B using a modification of the methodology proposed by Zhang et al. (2011). The implementation of the procedure is detailed below (see also the flowchart of Fig. 1, right):

0) $i = 0$.
1) Make $i = i + 1$, find the slip surface with minimum reliability index β (of those remaining) in Group B, and compute the vector of correlation coefficients $\boldsymbol{\rho}$ between such slip surface and all the slip surfaces in Group B (note that the selected slip surface has a correlation coefficient $\rho = 1$ with itself).
2) Exclude from Group B the slip surfaces which have correlation coefficients larger than a user-defined threshold, ρ_0, and send them into a new Subgroup C_i (Li et al. (2014) discussed how to select ρ_0 to balance accuracy and computational cost, suggesting that a value of about 0.8–0.9 is reasonable. In this study, $\rho_0 = 0.85$ is used).
3) Repeat Steps 1–2 until all the slip surfaces in Group B are classified into subgroups (i.e., until Group B is empty). The number of resultant C_i subgroups is referred to as m.
4) For each C_i subgroup, find the number of slip surfaces with the same β values. If there are more than one, reserve one of the slip surfaces with such β value and remove the others with the same β value from C_i (this is necessary to maintain a diversity in the population that explores the whole solution domain, and to avoid that the solution is trapped in a local minimum).
5) Sort, with ascending β values, the slip surfaces that remain in each C_i subgroup. The number of individuals remaining in each C_i subgroup is referred to as $N_{C,i}$.
6) Count the total number of slip surfaces that remain in all C_i subgroups. This is called N_{total}; i.e., $N_{\text{total}} = \sum_{i=1}^{m} N_{C,i}$. Erase Group A.
7) Select for survival approximately $N_{\text{ind,ini}}$ slip surfaces from all C_i subgroups, as follows: If $N_{\text{total}} \le N_{\text{ind,ini}}$ (remember that $N_{\text{ind,ini}} = 100$ is used herein), select all the slip surfaces in all C_i subgroups, and send them into a newly created Group A. If $N_{\text{total}} > N_{\text{ind,ini}}$, we start selecting the $N_{\text{select},i}$ 'top' ranked slip surfaces in each C_i (with slip surfaces sorted with ascending β values), where $N_{\text{select},i} = \text{round}$ ($N_{C,i} \times$ weight) and weight $= N_{\text{ind,ini}}/N_{\text{total}}$ (in addition, if $N_{C,i} < 3$, then $N_{\text{select},i} = N_{C,i}$). However, since this often selects too many slip surfaces from Subgroup C_1 (which contains the critical slip surface), an additional selection criterion is employed to balance 'exploration' (i.e., using parents from different C_i subgroups) and 'exploitation' (i.e., seeking the critical slip surface): $N_{\text{select},1}$ (for Subgroup C_1) is limited by $N_{\text{select},1} \le \text{round}\,(2 \times N_{\text{ind,ini}}/(N_{\text{layer}} + 1))$, and, for $i > 1$, $N_{\text{select},i} \le \text{round}\,(N_{\text{ind,ini}}/(N_{\text{layer}} + 1))$, where N_{layer} is the number of layers containing random variables. This results in $N_{\text{ind}} \approx N_{\text{ind,ini}}$ (but not necessarily $N_{\text{ind}} = N_{\text{ind,ini}}$) selected individuals that are sent to a newly created Group A.
8) Finally, the slip surface with minimum reliability index in each C_i subgroup is considered to be one of the m RSSs of the slope system for that specific generation. Note, however, that m can change as the algorithm evolves, although the RSSs will tend to improve with the number of generations so that, after a sufficiently large number of generations, the identified RSSs is expected to converge to the true RSSs of the slope.

Table 1
Case 1. Statistical parameters of random variables.

Layer	Random variable	Mean value	Standard deviation	Distribution type
1	C_1 (kPa)	10	2	Normal
	φ_1 (°)	12	3	Normal
2	C_2 (kPa)	40	8	Normal
	φ_2 (°)	0	0	–

3.6. Computing the slope's reliability

Once the RSSs for a given generation have been identified, they can be employed to estimate P_{fs}. Section 2.3 proposes one efficient and accurate approach, based on the complementary of the intersection of safe domains summarized by Eq. (3), and that only needs FORM (or SORM) information of the identified RSSs. But any other reliability method is also theoretically possible. For instance, simulation methods can also be employed at the expense of a higher computational cost.

3.7. Repeating the sequence

The procedure explained above can be repeated until convergence of the algorithm or until a user-defined number of generations, N_{gen}, has been completed ($N_{\text{gen}} = 400$ is employed in this work), so that the RSSs identified for such last iteration could be taken as representative of the slope system and of its associated probability of failure. The reliability information from the previous generation is useful to increase the computational efficiency of a subsequent generation: for each trial slip surface considered in a new generation (except the first one), the starting point needed by the iHLRF algorithm to compute its FORM-solution is taken from the FORM solution of the 'most similar' slip surface from the previous generation. (To assess 'similarity', we consider the number of layers intersected by each slip surface and the distance between their lowest vertices.) This strategy significantly reduces the number of iterations required for convergence of the iHLRF algorithm (to less than three for most trial slip surfaces), hence increasing efficiency.

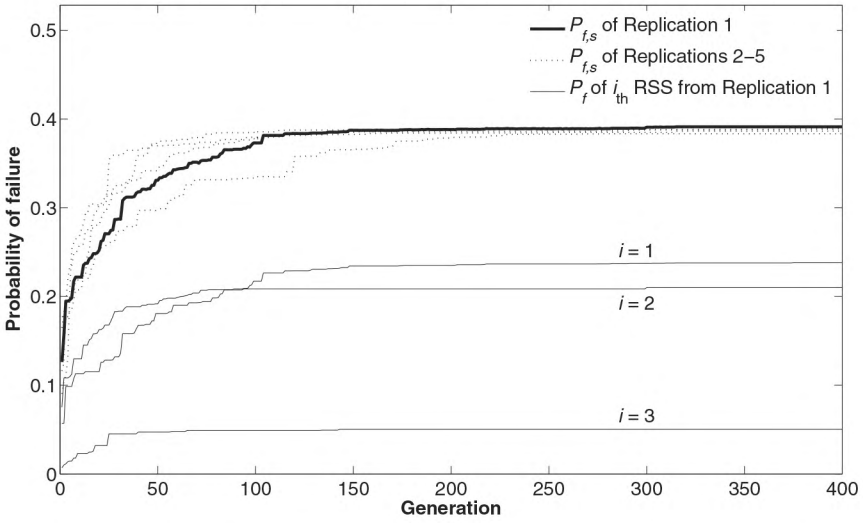

Fig. 4. Case 1. Evolution of $P_{f,s}$ for the five replications considered, and evolution of P_f of individual RSSs for Replication 1.

4. Case studies

Three typical layered soil slopes taken from the literature are employed to illustrate the ability of the suggested method to compute the reliability of a soil slope system. For each case, we conduct five replications with $N_{gen} = 400$ generations and $N_{ind,ini} = 100$ initial slip surfaces. Note that, when presenting results, the numbering of the five replications is changed so that they have a decreasing system probability of failure (videos showing convergence with the number of generations are provided as supplementary material, and the coordinates of nodes corresponding to the RSSs identified in Replication 1 for each case are listed in Appendix A).

The "allowable extreme nodes intervals" employed in each case are represented in the figures presenting their geometries. The entry angles of the slip surfaces in Cases 1, 2 and 3 (measured clockwise with respect to the X axis) are limited to be, respectively, within [30, 60], [45, 85] and [45, 60] intervals; and the exit angles (also measured clockwise with respect to the X axis) are limited to be within a [135, 200] interval in all cases.

4.1. Case 1

We start with a benchmark case consisting on an embankment resting on a soil foundation with horizontal surface; see Fig. 3. This case was originally proposed by Chowdhury and Xu (1995), and it has been also employed by many other researchers (see e.g., Ji and Low, 2012; Cho, 2013; Zhang et al., 2013). Table 1 lists the statistical properties of random variables employed to model the strength of both layers. They are all assumed to be independent and normally distributed.

Fig. 3 shows the three RSSs identified with the proposed GA-procedure in Replication 1 in this case. Fig. 4 shows, for the five replications, the evolution of $P_{f,s}$ with the number of generations; it also shows the evolution of the P_f of the individual RSSs. Fig. 5 lists the number of slip surfaces identified in each C_i subgroup in Replication 1 and their reliability indices; it also shows the correlation coefficients between the critical slip surface and all the slip surfaces from the subgroups.

Table 2 lists the reliability indices and the correlation matrix (computed by FORM) for the three RSSs identified in this case. Table 3 presents our computed $P_{f,s}$ results, using both the proposed linearization approach and MCS with the three RSSs; it also lists results computed with other methods proposed in the literature.

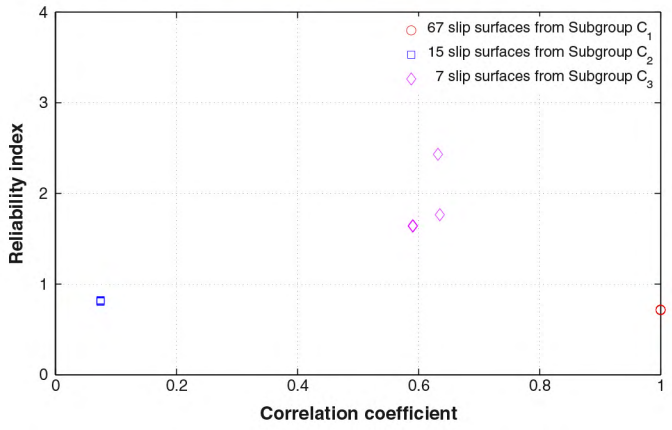

Fig. 5. Case 1. Correlation coefficients between the critical slip surface and all the slip surfaces from Replication 1.

4.2. Case 2

Another case, previously analyzed by Ji and Low (2012) and Zhang et al. (2013), is revisited here. Fig. 6 shows a slope with three layers with irregular shapes, in which it is more difficult to identify the RSSs. The cohesion, C, and friction angle, φ, of Layers 2 and 3 are considered to be independent normal random variables whose parameters are listed in Table 4 (following Zhang et al. (2013), the unit weights of soils in all layers are assumed to be 19.5 kN/m^3).

Fig. 6 also shows the four RSSs identified in Replication 1 in this case. Fig. 7 shows the evolution of computed probabilities of failure with the number of generations. Fig. 8 lists the number of slip surfaces in the four C_i subgroups identified in Replication 1; it also shows their reliability indices, as well as their correlation coefficients with the critical slip surface.

Table 2
Case 1. Reliability indices and correlation matrix for RSSs identified in Replication 1.

	β_1	β_2	β_3
	0.7127	0.8064	1.6414
R	1	2	3
1	1.0000	0.0746	0.5902
2	0.0746	1.0000	0.8490
3	0.5902	0.8490	1.0000

Table 3
Case 1. Results of system reliability analyses using different methods.

Method	LEM[a]	Slip surface shape	β_i	$\rho_{i,j}$	$P_{f,s}$	Reference
FORM-based	S	Fully specified	0.7127, 0.8064, 1.6414	See Table 2	0.3913	This study[b]
MCS[c]	S	Fully specified	0.7185, 0.8122, 1.6400	–	0.3880	This study[b]
Method in Ji and Low (2012)	S	Circular	0.8067, 0.8471	$\rho_{1,2} = 0.0854$	[0.317, 0.363]	Ji and Low (2012)
Method in Cho (2013)	S	Non-circular	0.791, 0.821	$\rho_{1,2} = 0.056$	0.3714	Cho (2013)
Method in Zhang et al. (2013)[d]	B	Circular	0.8099, 0.8705	Not reported	0.356	Zhang et al. (2013)

[a] Key: LEM = limit equilibrium method; S = Spencer; B = Bishop simplified.
[b] Results from Replication 1.
[c] $N = 30{,}000$, COV = 0.73%.
[d] The random variables follow lognormal distributions.

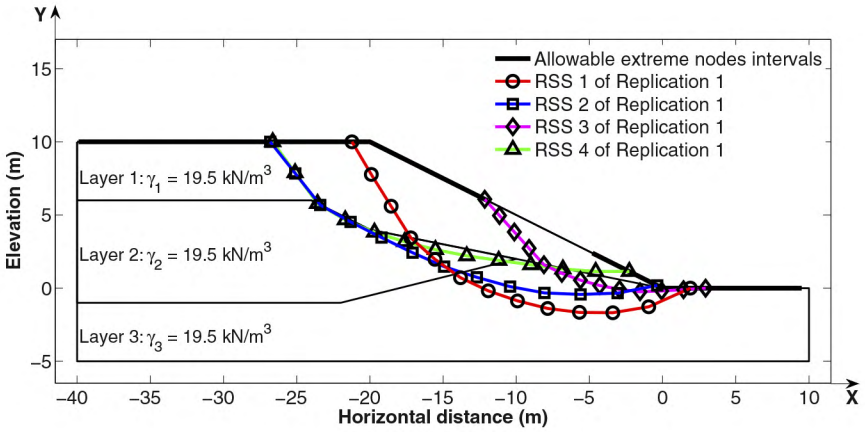

Fig. 6. Case 2. Geometry of a three layers soil slope and the RSSs identified in Replication 1.

Table 5 lists the FORM-reliability indices and the correlation matrix for the four identified RSSs. The values of $P_{f,s}$ computed using such RSSs are listed in Table 6; Table 6 also presents results reported by other researchers for this problem.

4.3. Case 3

Next, a 4-layer soil slope proposed by Zolfaghari et al. (2005) is employed to further test the proposed method with more complicated cases. Fig. 9 shows its geometry, characterized by an inclined weak planar seam. Eight strength parameters are considered as random variables with lognormal distributions; see Table 7. The cohesion, C, and friction angle, φ, of each layer are assumed to be negatively correlated, and the strength parameters of one layer are assumed to be independent of those of the other layers (i.e., $\rho_{C_i,\varphi_i} = -0.5$ and $\rho_{C_i,C_j} = \rho_{\varphi_i,\varphi_j} = \rho_{C_i,\varphi_j} = 0$ for $i, j = 1, \ldots, 4$ and $i \neq j$).

Fig. 9 also shows the six RSSs that are identified in Replication 1 in this case, whereas Fig. 10 shows the evolution of probabilities of failure with the number of generations. Fig. 11 shows the number of slip surfaces identified in each C_i subgroup, their reliability indices, and their correlation coefficients with the critical slip surface.

Table 4
Case 2. Statistical parameters of random variables.

Layer	Random variable	Mean value	Standard deviation	Distribution type
1	C_1 (kPa)	0	0	–
	φ_1 (°)	38.0	0	–
2	C_2 (kPa)	5.3	1.59	Normal
	φ_2 (°)	23.0	4.60	Normal
3	C_3 (kPa)	7.2	2.16	Normal
	φ_3 (°)	20.0	4.00	Normal

Table 8 lists the reliability indices (computed using FORM and SORM) and the correlation matrix for the six RSSs. Table 9 lists $P_{f,s}$ results computed by the different methods discussed herein.

5. Discussion of results

The RSSs identified in Cases 1 and 2, which are somewhat circular, are similar to the RSSs previously reported for these problems (see Ji and Low, 2012; Cho, 2013; Zhang et al., 2013). (Note, however, that the critical slip surface identified by Zhang et al. (2013) for Case 1 is very different, although both solutions are not directly comparable, as they considered lognormal random variables.) For Case 3 there are no results available for comparison in the literature, although Jurado-Piña and Jimenez (2014) demonstrated the advantages of the proposed GA to find slip surfaces with minimum F_S in this slope. In this case, the identified (probabilistic) critical slip surface (RSS 1) fulfills the expectations: it is a composite of arc and planar surfaces, intersecting Layers 1–3, and following the contact between the weak seam and the lower (and stronger) layer. Based on these observations, and on the previously demonstrated performance of the GA, we argue that the proposed method can identify good RSSs in a wide variety of layer geometries, including both cases in which circular and non-circular shapes are critical (even in the presence of weak seams).

In addition, results in Section 4 show that the proposed method provides good estimates of system reliability, which outperform other methods proposed in the literature for a wide variety of soil slopes for which a comparison is possible. The reason is that the proposed method, which naturally handles a wide range of slip surface geometries, finds very good critical slip surfaces that, in conjunction to the other RSSs identified, provide better estimations of $P_{f,s}$: compare, for instance, the critical $\beta_1 \approx 0.71$ computed using our approach in Case 1 (see Table 3) with the $\beta_1 \approx 0.79$–0.81 computed with other methods; or, for Case 2 (see Table 6), the $\beta_1 \approx 2.17$ computed with our method

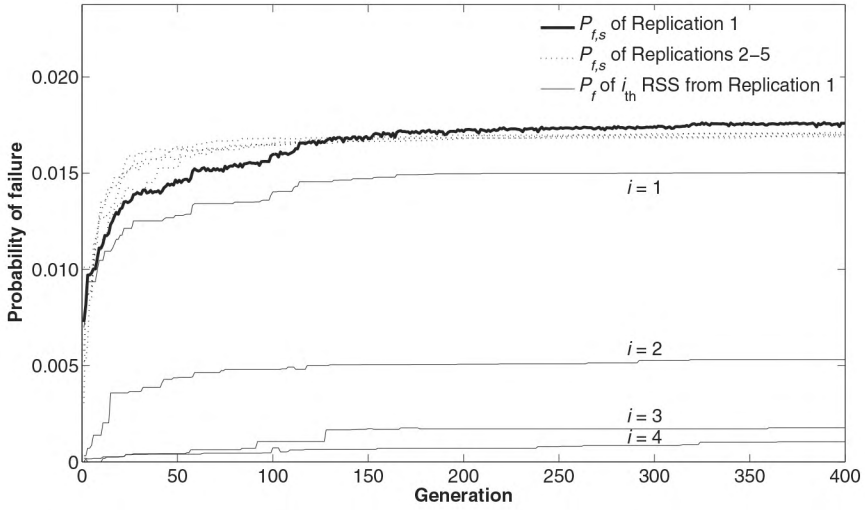

Fig. 7. Case 2. Evolution of $P_{f,s}$ for the five replications considered, and evolution of P_f of individual RSSs for Replication 1.

with the $\beta_1 \approx 2.36$–2.37 computed by other researchers using circular surfaces only (note, however, that some results may not be directly comparable: log-normally distributed random variables are considered for Case 1 in Zhang et al. (2013), and unit weights for Case 2 are not reported in Ji and Low (2012)).

Identifying very good critical slip surfaces is crucial for success because the system reliability is commonly dominated by just a few—indeed, often only one—RSSs. (It should be noted that this may not be the case for slopes where geotechnical spatial variability is explicitly considered.) For instance, although the contributions of RSSs 1 and 2 are both relevant in Case 1, with RSS 3 contributing little to the $P_{f,s}$, RSS 1 is the unique main contributor to $P_{f,s}$; in Cases 2 and 3, in which the contributions of the other RSSs are much lower (Note that comparing the reliability indices obtained by different methods for other RSSs (i.e., except the critical one) is irrelevant. This is because the β values of other RSSs are only indicators of their contribution to $P_{f,s}$; to compute their real contributions to $P_{f,s}$ with Eq. (3), we also need to consider their correlations with the critical slip surface, so that, for other RSSs which have the same β values, smaller correlation coefficients lead to more contributions to $P_{f,s}$, and vice-versa. In general, slip surfaces whose stability is controlled by the same layers are expected to be highly correlated, whereas slip surfaces whose stability is controlled by different layers are expected to have lower correlations.).

The discussion above illustrates that finding slip surfaces with a "reasonable" shape or with a shape "similar" to the critical one is not enough.

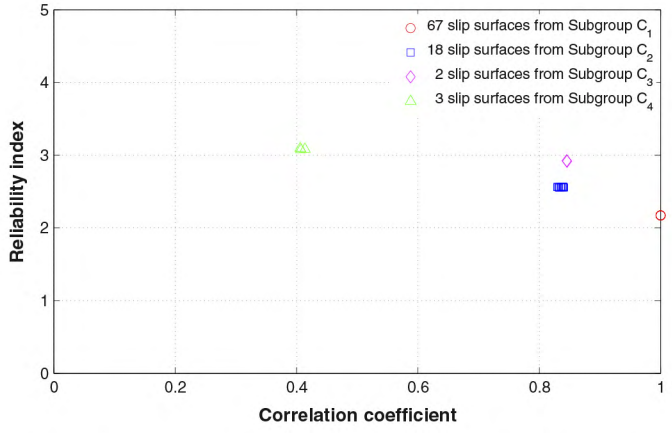

Fig. 8. Case 2. Correlation coefficients between the critical slip surface and all the slip surfaces from Replication 1.

This is one crucial limitation of methods considering circular solutions only (e.g., Ji and Low, 2012; Zhang et al., 2013); of "simulation-based" approaches (e.g., Ching et al., 2009; Li and Chu, 2014; Li et al., 2014), which do not guarantee that a good critical slip surface is included within the generated set that is later employed for simulation; or of other (weaker) "optimization" approaches (e.g., Ji and Low, 2012; Cho, 2013; Zhang et al., 2013) that do not guarantee a good critical slip surface solution.

But, because we are dealing with a system problem, we also need to consider other RSSs that, in addition to the critical slip surface, control the behavior of the slope. However, since the contribution of such other RSSs to $P_{f,s}$ decreases with their reliability (and with their correlation with the critical slip surface), the errors associated with not finding the best ith RSS (with $i > 1$) are often less relevant. That is why the proposed approach is designed (see Section 3.5) to automatically allocate 'resources' so that it balances "exploration" and "exploitation". Results presented above suggest that the strategy is adequate, as in all cases considered the number of slip surfaces in each C_i subgroup—which indicates the amount of 'resources' allocated to find the ith RSS—tends to decrease with i.

Meanwhile, one might be interested in how many RSSs are sufficient to represent the slope system. To the authors' knowledge, there is no specified rule that can predict this number. In general, it is expected that the number of RSSs required increases with the complexity of the slope system (e.g., with the number of layers and the number of random variables involved). However, our approach avoids this problem with the aid of ρ_0, so that it can automatically detect enough RSSs to estimate the probability of failure of the slope system. Theoretically, the number of RSSs identified for a given slope should increase as ρ_0 decreases, and vice-versa. Based on the results presented herein, the use of $\rho_0 = 0.85$—which is a tradeoff between accuracy and computational cost—is found to be acceptable.

Next, we discuss the errors associated with the linearization of the LSFs that is inherent to Eq. (3). In Cases 1 and 2, the $P_{f,s}$ computed by

Table 5
Case 2. Reliability indices and correlation matrix for RSSs identified in Replication 1.

	β_1	β_2	β_3	β_4
	2.1696	2.5546	2.9174	3.0773
R	1	2	3	4
1	1.0000	0.8327	0.8457	0.4073
2	0.8327	1.0000	0.6057	0.8447
3	0.8457	0.6057	1.0000	0.1813
4	0.4073	0.8447	0.1813	1.0000

Table 6
Case 2. Results of system reliability analyses using different methods.

Method	LEM[a]	Slip surface shape	β_i	$\rho_{i,j}$	$P_{f,s}$	Reference
FORM-based	S	Fully specified	2.1696, 2.5546, 2.9174, 3.0773	See Table 5	1.76%	This study[b]
MCS[c]	S	Fully specified	2.1775, 2.5530, 3.0068, 3.1149	–	1.72%	This study[b]
Method in Ji and Low (2012)[d]	S	Circular	2.3564, 2.4639	$\rho_{1,2} = 0.94$	[1.35%, 1.53%]	Ji and Low (2012)
Method in Zhang et al. (2013)	B	Circular	2.3698, 2.4893, 2.5364, 2.6356	Not reported	1.08%	Zhang et al. (2013)

[a] Key: LEM = limit equilibrium method; S = Spencer; B = Bishop simplified.
[b] Results from Replication 1.
[c] $N = 50{,}000$, COV = 3.38%.
[d] The unit weights of the three soil layers are not reported in Ji and Low (2012).

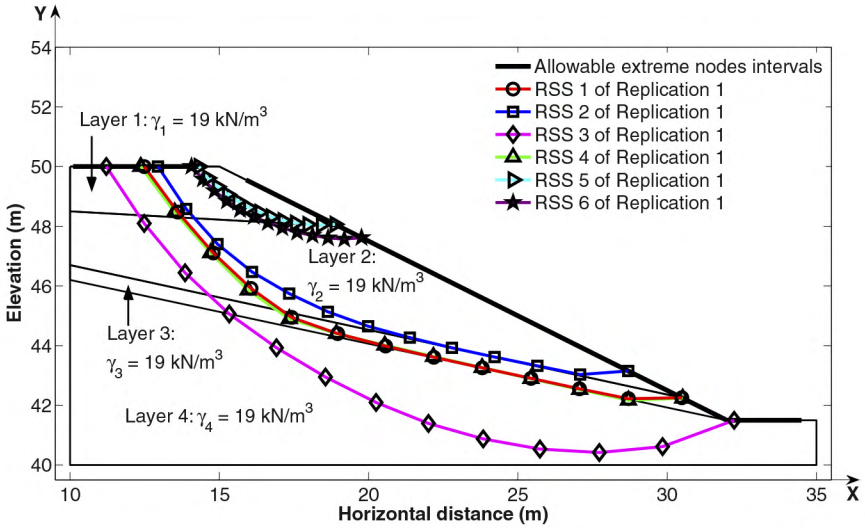

Fig. 9. Case 3. Geometry of a four layers soil slope with weak seam and the RSSs identified in Replication 1.

the linearization approach using FORM information agrees well with the MCS results computed using the same RSSs, hence showing that it can provide very good estimates of $P_{f,s}$ when the LSFs of the RSSs contributing most to $P_{f,s}$ are almost linear. (Remember that Eq. (3) would be exact for slopes in cohesive soils, computed using Bishop simplified method, and considering normal and uncorrelated variables.) However, in Case 3, the $P_{f,s}$ computed by the FORM-based linearization approach has a larger deviation with respect to the MCS result using the same RSSs, suggesting that their LSFs are more non-linear. To consider the non-linearity of the LSFs, the SORM is employed to compute a vector of 'equivalent' reliability indices (see Table 8), which are computed using the probabilities of failure given by SORM, $P_{f,\mathrm{SORM}}$, and the well-known relationship that $\beta = -\Phi^{-1}(P_f)$. This $\boldsymbol{\beta}_{\mathrm{SORM}}$ vector can then be employed, together with Eq. (3) and with the same correlation matrix of FORM, to compute an improved estimate of the system's reliability. Table 9 shows that the solution significantly improves using such SORM-based information, providing a $P_{f,s}$ estimate with a very small deviation with respect to the MCS result. And, of course, using the proposed linearization approach is not a requirement of the methodology; for instance, as discussed in Section 3.6, it is always possible, at the expense of a higher computational cost (see Table 9), to use simulation methods to compute $P_{f,s}$ using the RSSs identified with the proposed approach.

Finally, results in Section 4 show that the method proposed herein can be considered 'robust', as replications employed in all example cases converge to very similar estimates of the $P_{f,s}$ before the 400 generations considered. And, even though it is not possible to directly compare with the convergence of other methods in the literature for which results have not been reported, the algorithms have been designed having efficiency in mind. For instance (see Section 3.7), FORM solutions of individuals from previous generations in the GA are employed to facilitate good starting points for the iterative iHLRF algorithm that evaluates the reliability of new individuals. And, given the importance of finding good critical slip surfaces discussed above, another computational advantage of the proposed approach is that it only needs to solve the optimization problem of finding RSSs once, hence representing a conceptual improvement with respect to other simulation-based approaches that need to solve such optimization problem—which is a challenging task if good critical slip surfaces are needed, even if they are deterministic—for each set of simulated random variables (i.e., for each simulation conducted).

Table 7
Case 3. Statistical parameters of random variables.

Layer	Random variable	Mean value	Standard deviation	Distribution type
1	C_1 (kPa)	18	9.0	Lognormal
	φ_1 (°)	16	4.8	Lognormal
2	C_2 (kPa)	20	10.0	Lognormal
	φ_2 (°)	14	4.2	Lognormal
3	C_3 (kPa)	12	3.6	Lognormal
	φ_3 (°)	10	2.0	Lognormal
4	C_4 (kPa)	20	10.0	Lognormal
	φ_4 (°)	18	5.4	Lognormal

6. Conclusions

We propose a new approach, based on the use of a GA specifically designed for slope stability problems; and on modifications to the method suggested in Zhang et al. (2011) to (*i*) systematically identify the fully specified representative slip surfaces (RSSs) of slopes in layered soil and (*ii*) to compute their (series) system reliability. The approach takes advantage of the system aspects of the problem and, in particular, of the

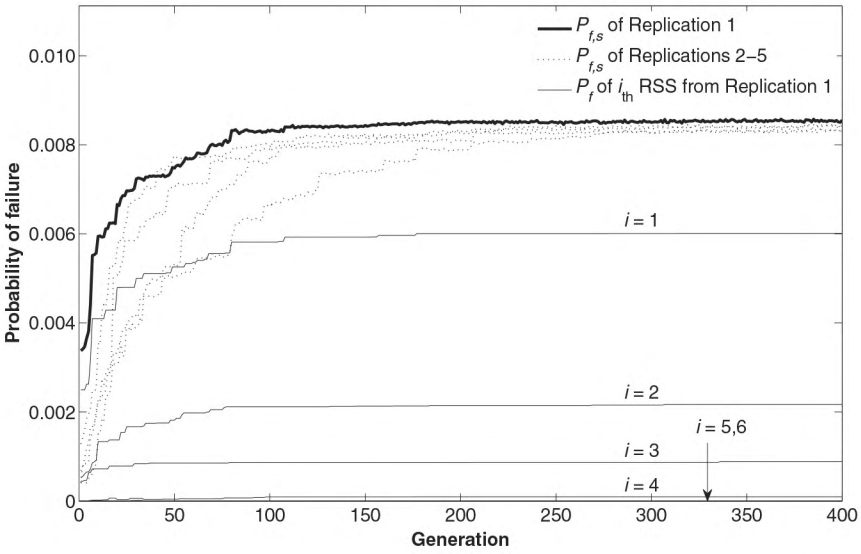

Fig. 10. Case 3. Evolution of $P_{f,s}$ for the five replications considered, and evolution of P_f of individual RSSs for Replication 1.

correlation that exists between slip surfaces, which makes a few "representative slip surfaces" to explain most of the system's probability of failure. To increase computational efficiency, it also uses the observation that many slope stability LSFs are quite linear; note, however, that this is not a requirement of the approach, since simulations methods can be employed, at the expense of a higher computational cost, to completely capture the non-linearity of the LSFs associated to the slope's RSSs.

Three example cases with different layered soil slopes have been employed to test the proposed method. The main conclusions of such analysis are summarized below:

1) The proposed method is able to identify good RSSs, providing estimates of the system probability of failure that improve those reported in previous studies in a wide variety of layered soil slopes.
2) A wide range of slip surface geometries are naturally handled with the GA employed to identify the RSSs. The ability to use such flexible fully specified slip surfaces, in conjunction with the good optimization performance of the GA employed, enables the proposed method to identify very good critical slip surfaces of various shapes and in different positions, even when a weak seam exists. In conjunction with the proposed procedure to identify the RSSs, this has been identified as a crucial strength of the proposed approach, as identifying good critical slip surfaces is one key aspect for success of these RSS-based approaches.

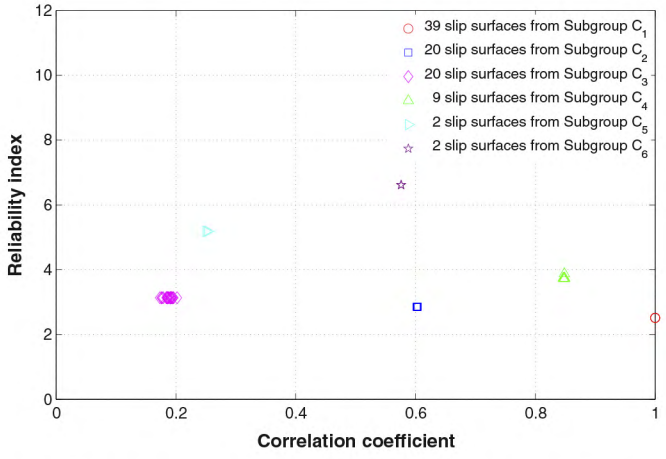

Fig. 11. Case 3. Correlation coefficients between the critical slip surface and all the slip surfaces from Replication 1.

3) The proposed approach avoids the computational cost typically associated to conventional reliability methods based on simulation (i.e., MCS, IS or subset simulation). Instead, it uses FORM to approximately compute the reliability of trial slip surfaces. On the other hand, it searches all the RSSs simultaneously only once, whereas other methods that use simulation to obtain unbiased $P_{f,s}$ estimators need to search the critical slip surface for (almost) all simulations conducted.
4) The proposed method is robust. All cases studied converge to very similar estimates of the system probability of failure before the 400 generations considered.

Table 8
Case 3. Reliability indices and correlation matrix of FORM and SORM for RSSs identified in Replication 1.

FORM						
β	2.5115	2.8524	3.1266	3.7315	5.1830	6.6133
SORM						
β	2.7601	3.0260	3.3623	4.0822	5.2837	6.8200
Correlation matrix						
R	1	2	3	4	5	6
1	1.0000	0.6023	0.1908	0.8476	0.2505	0.5762
2	0.6023	1.0000	0.2386	0.5797	0.2044	0.8443
3	0.1908	0.2386	1.0000	0.6367	0.1038	0.2327
4	0.8476	0.5797	0.6367	1.0000	0.2385	0.5514
5	0.2505	0.2044	0.1038	0.2385	1.0000	0.6864
6	0.5762	0.8443	0.2327	0.5514	0.6864	1.0000

Table 9
Case 3. Results of system reliability analyses from Replication 1.

Method	$P_{f,s}$	Computational time (seconds)[a]
FORM-based	0.861%	4.7
SORM-based	0.429%	246.1
MCS[b]	0.420%	41,439.4

[a] Time needed to compute the system probability of failure only, based on the same identified RSSs.
[b] $N = 50{,}000$, COV = 6.89%.

5) The linearization approach employed to compute the system probability of failure is simple, efficient, and accurate. It only needs results (vector of reliability indices and unit direction vectors) provided by FORM. And, when the LSFs contributing most to the system probability of failure become highly nonlinear, their estimates can be further improved using SORM-based information or, at the expense of a higher computational cost, using simulation methods with the identified RSSs.

Acknowledgments

The first author is supported by China Scholarship Council (CSC), under grant 2011709051; and, for insurance coverage, by Fundación José Entrecanales Ibarra. Dr. Solange Regina dos Santos kindly provided his MATLAB codes for the HLRF-based FORM algorithms. Their support is greatly appreciated.

Appendix A

The coordinates of nodes corresponding to the RSSs identified in Replication 1 for each example case considered.

Table A.1
Case 1.

Node	RSS 1		RSS 2		RSS 3	
	X (m)	Y (m)	X (m)	Y (m)	X (m)	Y (m)
1	25.15	17.58	31.77	20.00	29.92	19.96
2	28.16	13.64	33.54	17.83	31.78	17.83
3	31.18	9.75	35.42	15.97	33.77	16.08
4	34.30	6.43	37.40	14.40	35.79	14.43
5	37.53	3.68	39.47	13.09	37.89	13.02
6	40.89	1.73	41.63	12.02	40.07	11.85
7	44.38	0.53	43.86	11.16	42.27	10.77
8	48.00	0.05	46.20	10.63	44.51	9.79
9	51.72	0.14	48.61	10.26	47.05	9.72
10	55.60	1.15	51.08	10.07	49.66	9.89
11	59.70	3.42	53.59	10.01	52.28	10.10
12	63.94	6.46	56.15	10.08	54.92	10.33
13	68.27	10.00	58.82	10.47	57.67	10.93

Table A.2
Case 2.

Node	RSS 1		RSS 2		RSS 3		RSS 4	
	X (m)	Y (m)	X (m)	Y (m)	X (m)	Y (m)	X (m)	Y (m)
1	−21.22	10.00	−26.80	10.00	−12.15	6.08	−26.64	10.00
2	−19.90	7.77	−25.10	7.84	−11.14	4.96	−25.11	7.89
3	−18.55	5.60	−23.39	5.69	−10.13	3.84	−23.58	5.78
4	−17.20	3.44	−21.31	4.53	−9.12	2.72	−21.68	4.67
5	−15.55	1.97	−19.21	3.46	−8.11	1.60	−19.69	3.82
6	−13.81	0.71	−17.08	2.42	−6.88	1.01	−17.63	3.18
7	−11.91	−0.18	−14.93	1.47	−5.61	0.54	−15.53	2.63
8	−9.91	−0.87	−12.69	0.74	−4.30	0.18	−13.38	2.21
9	−7.85	−1.39	−10.42	0.11	−2.94	−0.09	−11.20	1.90
10	−5.68	−1.66	−8.08	−0.33	−1.55	−0.25	−9.01	1.60
11	−3.40	−1.68	−5.61	−0.43	−0.06	−0.19	−6.81	1.31
12	−0.94	−1.27	−3.07	−0.34	1.43	−0.10	−4.58	1.14
13	1.90	0.00	−0.37	0.18	2.94	0.00	−2.28	1.14

Table A.3
Case 3.

Node	RSS 1		RSS 2		RSS 3		RSS 4		RSS 5		RSS 6	
	X (m)	Y (m)	X (m)	Y (m)	X (m)	Y (m)	X (m)	Y (m)	X (m)	Y (m)	X (m)	Y (m)
1	12.48	50.00	12.95	50.00	11.21	50.00	12.37	50.00	14.32	50.00	14.07	50.00
2	13.61	48.48	13.89	48.58	12.48	48.10	13.50	48.48	14.61	49.62	14.45	49.58
3	14.79	47.11	14.94	47.40	13.85	46.44	14.71	47.11	14.93	49.32	14.84	49.19
4	16.06	45.91	16.09	46.47	15.33	45.06	15.96	45.86	15.27	49.07	15.26	48.84
5	17.42	44.95	17.34	45.74	16.91	43.93	17.34	44.90	15.62	48.84	15.69	48.56
6	18.97	44.40	18.63	45.13	18.56	42.95	18.92	44.40	15.98	48.63	16.15	48.32
7	20.57	43.99	19.98	44.65	20.25	42.09	20.54	44.01	16.36	48.47	16.63	48.12
8	22.18	43.61	21.38	44.27	22.01	41.39	22.17	43.63	16.74	48.31	17.11	47.95
9	23.81	43.25	22.79	43.92	23.84	40.88	23.80	43.26	17.13	48.19	17.61	47.80
10	25.44	42.90	24.22	43.62	25.74	40.53	25.43	42.89	17.55	48.11	18.12	47.69
11	27.06	42.55	25.65	43.32	27.73	40.42	27.07	42.53	17.97	48.06	18.64	47.61
12	28.70	42.22	27.08	43.03	29.85	40.62	28.70	42.17	18.42	48.04	19.18	47.57
13	30.49	42.25	28.70	43.15	32.24	41.50	30.52	42.24	18.87	48.06	19.76	47.62

Appendix B. Supplementary data

Supplementary data to this article can be found online at http://dx.doi.org/10.1016/j.enggeo.2015.04.026.

References

Ching, J., Phoon, K., Hu, Y., 2009. Efficient evaluation of reliability for slopes with circular slip surfaces using importance sampling. J. Geotech. Geoenviron. 135, 768–777. http://dx.doi.org/10.1061/(ASCE)GT.1943-5606.0000035.

Ching, J., Phoon, K., Hu, Y., 2010. Observations on limit equilibrium-based slope reliability problems with inclined weak seams. J. Eng. Mech. 136, 1220–1233. http://dx.doi.org/10.1061/(ASCE)EM.1943-7889.0000160.

Cho, S.E., 2009. Probabilistic stability analyses of slopes using the ANN-based response surface. Comput. Geotech. 36, 787–797. http://dx.doi.org/10.1016/j.compgeo.2009.01.003.

Cho, S.E., 2013. First-order reliability analysis of slope considering multiple failure modes. Eng. Geol. 154, 98–105. http://dx.doi.org/10.1016/j.enggeo.2012.12.014.

Chowdhury, R.N., Xu, D.W., 1993. Rational polynomial technique in slope-reliability analysis. J. Geotech. Eng. 119, 1910–1928. http://dx.doi.org/10.1061/(ASCE)0733-9410(1993)119:12(1910).

Chowdhury, R.N., Xu, D.W., 1995. Geotechnical system reliability of slopes. Reliab. Eng. Syst. Saf. 47, 141–151. http://dx.doi.org/10.1016/0951-8320(94)00063-T.

Cornell, C.A., 1971. First-order uncertainty analysis of soils deformation and stability. Proceeding of the 1st International Conference on Application of Statistics and Probability to Soil and Structural Engineering, Hong Kong, pp. 130–143.

Der Kiureghian, A., 2005. First- and second-order reliability methods. In: Nikolaidis, E., Ghiocel, D.M., Singhal, S. (Eds.), Chapter 14 in Engineering Design Reliability Handbook. CRC Press, Boca Raton, FL.

Duncan, J.M., Song, K.S., 1984. SLOPE8R: A Computer Program for Slope Stability Analysis With Non-Circular Slip Surfaces. Technical Report. Department of Civil Engineering, University of California, Berkeley, CA.

Duncan, J.M., Wright, S.G., 2005. Soil Strength and Slope Stability. John Wiley & Sons.

Greco, V., 1996. Efficient Monte Carlo technique for locating critical slip surface. J. Geotech. Eng. 122, 517–525. http://dx.doi.org/10.1061/(ASCE)0733-9410(1996)122:7(517).

Griffiths, D., Fenton, G., 2004. Probabilistic slope stability analysis by finite elements. J. Geotech. Geoenviron. 130, 507–518. http://dx.doi.org/10.1061/(ASCE)1090-0241(2004)130:5(507).

Hasofer, A.M., Lind, N.C., 1974. Exact and invariant second moment code format. J. Eng. Mech. Div. 100, 111–121.

Hohenbichler, M., Rackwitz, R., 1982. First-order concepts in system reliability. Struct. Saf. 1, 177–188. http://dx.doi.org/10.1016/0167-4730(82)90024-8.

Hong, H., Roh, G., 2008. Reliability evaluation of earth slopes. J. Geotech. Geoenviron. 134, 1700–1705. http://dx.doi.org/10.1061/(ASCE)1090-0241(2008)134:12(1700).

Huang, J.S., Griffiths, D.V., Fenton, G.A., 2010. System reliability of slopes by RFEM. Soils Found. 50, 343–353.

Ji, J., Low, B., 2012. Stratified response surfaces for system probabilistic evaluation of slopes. J. Geotech. Geoenviron. 138, 1398–1406. http://dx.doi.org/10.1061/(ASCE)GT.1943-5606.0000711.

Jurado-Piña, R., Jimenez, R., 2014. A genetic algorithm for slope stability analyses with concave slip surfaces using custom operators. Eng. Optim. 1–20. http://dx.doi.org/10.1080/0305215X.2014.895339.

Kim, J.Y., Lee, S.R., 1997. An improved search strategy for the critical slip surface using finite element stress fields. Comput. Geotech. 21, 295–313. http://dx.doi.org/10.1016/S0266-352X(97)00027-X.

Krahn, J., 2004. Stability Modeling With SLOPE/W: An Engineering Methodology. GOE-SLOPE/W International Ltd., Calgary, Alberta, Canada.

Li, L., Chu, X., 2014. Multiple response surfaces for slope reliability analysis. Int. J. Numer. Anal. Methods in Geomech. http://dx.doi.org/10.1002/nag.2304.

Li, Y.-C., Chen, Y.-M., Zhan, T.L.T., Ling, D.-S., Cleall, P.J., 2010. An efficient approach for locating the critical slip surface in slope stability analyses using a real-coded genetic algorithm. Can. Geotech. J. 47, 806–820. http://dx.doi.org/10.1139/T09-124.

Li, L., Wang, Y., Cao, Z., Chu, X., 2013. Risk de-aggregation and system reliability analysis of slope stability using representative slip surfaces. Comput. Geotech. 53, 95–105. http://dx.doi.org/10.1016/j.compgeo.2013.05.004.

Li, L., Wang, Y., Cao, Z., 2014. Probabilistic slope stability analysis by risk aggregation. Eng. Geol. 176, 57–65.

Low, B.K., Zhang, J., Tang, W.H., 2011. Efficient system reliability analysis illustrated for a retaining wall and a soil slope. Comput. Geotech. 38, 196–204. http://dx.doi.org/10.1016/j.compgeo.2010.11.005.

Oka, Y., Wu, T., 1990. System reliability of slope stability. J. Geotech. Eng. 116, 1185–1189. http://dx.doi.org/10.1061/(ASCE)0733-9410(1990)116:8(1185).

Phoon, K.K., 2008. Reliability-based Design in Geotechnical Engineering: Computations and Applications. In: Phoon, K.K. (Ed.), Taylor & Francis, New York.

Rackwitz, R., Flessler, B., 1978. Structural reliability under combined random load sequences. Comput. Struct. 9, 489–494. http://dx.doi.org/10.1016/0045-7949(78)90046-9.

Santos, S.R., Matioli, L.C., Beck, A.T., 2012. New optimization algorithms for structural reliability analysis. Comput. Model. Eng. Sci. 83, 23–56.

Sun, J., Li, J., Liu, Q., 2008. Search for critical slip surface in slope stability analysis by spline-based GA method. J. Geotech. Geoenviron. 134, 252–256. http://dx.doi.org/10.1061/(ASCE)1090-0241(2008)134:2(252).

Wang, Y., Cao, Z., Au, S.-K., 2011. Practical reliability analysis of slope stability by advanced Monte Carlo simulations in a spreadsheet. Can. Geotech. J. 48, 162–172. http://dx.doi.org/10.1139/T10-044.

Zeng, P., Jimenez, R., 2014. An approximation to the reliability of series geotechnical systems using a linearization approach. Comput. Geotech. 62, 304–309. http://dx.doi.org/10.1016/j.compgeo.2014.08.007.

Zhang, Y., Der Kiureghian, A., 1995. Two improved algorithms for reliability analysis. In: Rackwitz, R., Augusti, G., Borri, A. (Eds.), Reliability and Optimization of Structural Systems. Springer US, pp. 297–304.

Zhang, J., Zhang, L.M., Tang, W.H., 2011. New methods for system reliability analysis of soil slopes. Can. Geotech. J. 48, 1138–1148. http://dx.doi.org/10.1139/t11-009.

Zhang, J., Huang, H.W., Juang, C.H., Li, D.Q., 2013. Extension of Hassan and Wolff method for system reliability analysis of soil slopes. Eng. Geol. 160, 81–88. http://dx.doi.org/10.1016/j.enggeo.2013.03.029.

Zolfaghari, A.R., Heath, A.C., McCombie, P.F., 2005. Simple genetic algorithm search for critical non-circular failure surface in slope stability analysis. Comput. Geotech. 32, 139–152. http://dx.doi.org/10.1016/j.compgeo.2005.02.001.